General Simulations of Excited Quartet Spectra with Electron-Spin Polarizations: The Excited Multiplet States of (Tetraphenylporphinato)zinc(II) Coordinated by *p*- or *m*-Pyridyl Nitronyl Nitroxides

Kazuyuki Ishii,[†] Jun-ichi Fujisawa,[‡] Atsushi Adachi,[†] Seigo Yamauchi,[‡] and Nagao Kobayashi*[,†]

Contribution from the Department of Chemistry, Graduate School of Science, and Institute for Chemical Reaction Science, Tohoku University, Sendai 980-8578, Japan

Received September 8, 1997. Revised Manuscript Received January 4, 1998

Abstract: The excited multiplet states of (tetraphenylporphinato)zinc(II) (ZnTPP) coordinated by *p*-pyridyl nitronyl nitroxide (*p*-nitpy), ZnTPP−*p*-nitpy, and of ZnTPP coordinated by *m*-nitpy, ZnTPP−*m*-nitpy, were studied by time-resolved electron paramagnetic resonance (TREPR). The TREPR spectra observed at 20 K and 0.5 μs after laser excitation were assigned to the lowest excited doublet (D_1) and quartet (Q_1) states for both the para and meta complexes. The TREPR spectra of the Q_1 state with electron-spin polarization (ESP) were well simulated for the first time. From the spectral simulation, it was established in general that the ESP in the Q_1 state was interpreted by selective intersystem crossing (ISC), which was generated by spin−orbit coupling (SOC) between the excited doublet states and the eigenfunctions of the Q_1 state in zero magnetic field. The TREPR spectra of the ZnTPP−nitpy systems were interpreted by selective ISC to the $|\pm^1/_2\rangle$ spin sublevels of the Q_1 state, which originated from SOC due to the zinc ion. The ESP in the D_1 state was interpreted by the difference between the internal conversion rate to the $|+^1/_2\rangle$ spin sublevel and that to the $|-^1/_2\rangle$ spin sublevel.

Introduction

Time-resolved electron paramagnetic resonance (TREPR) is a useful method by which many kinds of photoreaction intermediates, radicals and photoexcited triplet species, have been investigated.[1−5] Although photoexcited triplet species, which are diamagnetic in the ground state, have been intensively examined,[1,6,7] there have been few TREPR studies on photoexcited multiplet species, which are paramagnetic in the ground state.[8,9] If these excited multiplet states were observable, we would be able to obtain novel information such as electron-spin polarizations (ESP) and various EPR parameters, as for the excited triplet states.

Some applications of TREPR to photoexcited multiplet states are considered as follows. Firstly, elucidation of the excited states of paramagnetic metallo complexes will give information on the electronic properties in the excited state, which are also important for evaluation of the magnetic properties in the ground state. Further, the interaction between an excited triplet molecule and various paramagnetic species, radicals or excited triplet species, can also be evaluated. The excited triplet molecules are known to be quenched by paramagnetic species due to a change in the spin multiplicity. It is therefore significant for the evaluation of such interaction to observe pairs constituted by paramagnetic species. Although the TREPR method was efficient enough to evaluate them, there had been few direct observations of such pairs except radical pairs.[4,5]

Recently, we reported the first TREPR spectra of the excited doublet and quartet states for (tetraphenylporphinato)zinc(II) (ZnTPP) coordinated by *p*-pyridyl nitronyl nitroxide (*p*-nitpy), ZnTPP−*p*-nitpy, in the solid state.[10] These spectra were assigned and analyzed using the *g* values and zero-field splittings (zfs). However, the ESP was not discussed, since a simulation method for the excited quartet spectra with ESP had not been established at that time. It is therefore important to develop a

* To whom correspondence should be addressed.
[†] Department of Chemistry, Graduate School of Science.
[‡] Institute for Chemical Reaction Science.

(1) (a) Kim, S. S.; Weissman, S. I. *J. Mag. Reson.* **1976**, *24*, 167. (b) Kim, S. S.; Weissman, S. I. *Rev. Chem. Intermed.* **1979**, *3*, 107.
(2) (a) Wong, S. K.; Hutchinson, D. A.; Wan, J. K. S. *J. Chem. Phys.* **1973**, *58*, 985. (b) Pedersen, J. B.; Freed, J. H. *J. Chem. Phys.* **1975**, *62*, 1706.
(3) (a) Adrian, F. J. *J. Chem. Phys.* **1971**, *54*, 3918. (b) Adrian, F. J.; Monchick, L. *J. Chem. Phys.* **1979**, *71*, 2600.
(4) (a) Sakaguchi, Y.; Hayashi, H.; Murai, H.; I'Haya, Y. J. *Chem. Phys. Lett.* **1984**, *110*, 275. (b) Sakaguchi, Y.; Hayashi, H.; Murai, H.; I'Haya, Y. J. *Chem. Phys. Lett.* **1985**, *120*, 401.
(5) (a) Buckley, C. D.; Hunter, D. A.; Hore, P. J.; McLauchlan, K. A. *Chem. Phys. Lett.* **1987**, *135*, 307. (b) Tominaga, K.; Yamauchi, S.; Hirota, N. *J. Chem. Phys.* **1990**, *92*, 5175.
(6) (a) Murai, H.; Imamura, T.; Obi, K. *Chem. Phys. Lett.* **1982**, *87*, 295. (b) Murai, H.; Imamura, T.; Obi, K. *J. Phys. Chem.* **1982**, *86*, 3279. (c) Terazima, M.; Yamauchi, S.; Hirota, N. *Chem. Phys. Lett.* **1983**, *98*, 145.
(7) (a) Chandrashekar, T. K.; van Willigen, H.; Ebersole, M. H. *J. Phys. Chem.* **1984**, *88*, 4326. (b) Gonen, O.; Levanon, H. *J. Phys. Chem.* **1985**, *89*, 1637. (c) Ishii, K.; Yamauchi, S.; Ohba, Y.; Iwaizumi, M.; Uchiyama, I.; Hirota, N.; Maruyama, K.; Osuka, A. *J. Phys. Chem.* **1994**, *98*, 9431. (d) Ishii, K.; Ohba, Y.; Iwaizumi, M.; Yamauchi, S. *J. Phys. Chem.* **1996**, *100*, 3839.
(8) Kothe, G.; Kim, S. S.; Weissman, S. I. *Chem. Phys. Lett.* **1980**, *71*, 445.
(9) Corvaja, C.; Maggini, M.; Prato, M.; Scorrano, G.; Venzin, M. *J. Am. Chem. Soc.* **1995**, *117*, 8857.
(10) Ishii, K.; Fujisawa, J.; Ohba, Y.; Yamauchi, S. *J. Am. Chem. Soc.* **1996**, *118*, 13079.

S0002-7863(97)03146-6 CCC: $15.00
Published on Web 03/21/1998

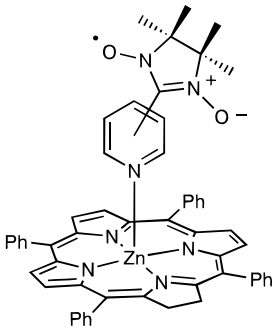

Figure 1. Molecular structure of the ZnTPP−nitpy system.

method for evaluating the excited quartet spectra not only for investigating the origin of the ESP in our system but also for the development of the TREPR study on the excited multiplet state.

For these reasons, we have attempted to simulate the excited quartet spectra with ESP. In this report, we have examined ZnTPP−*p*-nitpy and ZnTPP−*m*-nitpy (Figure 1). These paramagnetic complexes were discussed in terms of the following themes: (1) we simulated the photoexcited quartet spectra and proposed an ESP mechanism for the general excited quartet state. Further, the ESP of the excited doublet state was also considered. (2) The origin of the ESP in our system was investigated by considering the molecular orbitals. (3) The obtained EPR parameters, zfs and *g* values, were evaluated from the differences between ZnTPP−*p*-nitpy and ZnTPP−*m*-nitpy.

Experimental Section

ZnTPP, *p*-nitpy, and *m*-nitpy were synthesized by methods described elsewhere.[10,11] Spectral-grade toluene was used as the solvent for all measurements. The degree of coordination was checked by changes in the absorption spectra. The equilibrium constant of coordination at room temperature was estimated as $5 \times 10^3\ M^{-1}$ for both the para and meta complexes.[10,11] All samples were dearated by the freeze−pump−thaw method and were examined under conditions where the coordination was >96% even at room temperature.

Absorption spectra were measured with a Shimadzu UV-240 spectrometer. Emission spectra were measured at 77 K with a Hitachi 850 fluorescence spectrometer. Emission lifetimes at 80 K were measured through a Nikon G250 monochromator by a Hamamatsu Photonics R928 photomultiplier upon excitation by a Spectra Physics MOPO-710 broad-band OPO laser pumped with a Spectra Physics GCR-170-10 Nd:YAG laser. The emission signals were converted on Iwatsu DM-7200 digital memory. TREPR measurements were carried out at 20 K on a JEOL JES-FE2XG EPR spectrometer with a modified fast amplifier or on a Bruker ESP 300E spectrometer. Steady-state EPR measurements were made using the same apparatus. For the TREPR measurements, samples were excited at 585 nm by a Lambda Physik LPD3000 dye laser pumped with a Lambda Physik LPX100i excimer laser or by a Lumonics HD-500 dye laser pumped with a Lumonics EX 500 excimer laser. The TREPR signals from the EPR unit were integrated by an NF BX-531 boxcar integrator or by a LeCroy 9450A oscilloscope. For the EPR and emission lifetime measurements, the temperature was controlled using an Oxford ESR 900 cold gas flow system.

Simulation Method for Excited Quartet Spectra

The ESP in the excited triplet state is interpreted by the selective intersystem crossing (ISC) stimulated by the intramolecular spin−orbit coupling (SOC). We therefore tried to simulate the ESP of the excited quartet spectra with reference to the case of the excited triplet state.

Chart 1

$$\begin{array}{c} \\ \langle Q,+^3/_2'| \\ \langle Q,+^1/_2'| \\ \langle Q,-^1/_2'| \\ \langle Q,-^3/_2'| \end{array} \begin{array}{c} \begin{array}{cccc} |Q,+^3/_2'\rangle & |Q,+^1/_2'\rangle & |Q,-^1/_2'\rangle & |Q,-^3/_2'\rangle \end{array} \\ \begin{pmatrix} D + {}^3/_2 G_z & (\sqrt{3}/2)G_- & \sqrt{3}E & 0 \\ (\sqrt{3}/2)G_+ & -D + {}^1/_2 G_z & G_- & \sqrt{3}E \\ \sqrt{3}E & G_+ & -D + {}^1/_2 G_z & (\sqrt{3}/2)G_- \\ 0 & \sqrt{3}E & (\sqrt{3}/2)G_+ & D - {}^3/_2 G_z \end{pmatrix} \end{array}$$

$|Q,+^3/_2'\rangle = |\alpha\alpha\alpha\rangle$, $|Q,+^1/_2'\rangle = \{|\alpha\alpha\beta\rangle + |\alpha\beta\alpha\rangle + |\beta\alpha\alpha\rangle\}/\sqrt{3}$,

$|Q,-^1/_2'\rangle = \{|\alpha\beta\beta\rangle + |\beta\alpha\beta\rangle + |\beta\beta\alpha\rangle\}/\sqrt{3}$, $|Q,-^3/_2'\rangle = |\beta\beta\beta\rangle$

$G_z = g\beta B_{M_s \Leftrightarrow M_s+1} \cos\theta$, $G_\pm = g\beta B_{M_s \Leftrightarrow M_s+1} (\sin\theta \cos\phi \pm i \sin\theta \sin\phi)$

[a] D and E values are zero-field splitting parameters; θ and ϕ are the angle between the vector along the external magnetic field ($\vec{B}_{M_s \Leftrightarrow M_s+1}$) and the fine structure axis z and the angle between $\vec{B}_{M_s \Leftrightarrow M_s+1}$ and the fine structure axis x, respectively; $|Q,M_s'\rangle$ ($M_s = -^3/_2, -^1/_2, {}^1/_2$, and $^3/_2$) are basic functions, which are eigenfunctions when $B_{M_s \Leftrightarrow M_s+1} = E = 0$.

The excited quartet spectra were calculated using the following spin Hamiltonian, H_{spin}.

$$H_{spin} = \boldsymbol{g}\beta\boldsymbol{B}\boldsymbol{S} + \boldsymbol{S}\boldsymbol{D}\boldsymbol{S} = \boldsymbol{g}\beta\boldsymbol{B}\boldsymbol{S} + D[S_z^2 - S(S+1)/3] + E(S_x^2 - S_y^2) \quad (1)$$

Here, β is the Bohr magneton, $\boldsymbol{S}$ is the total electron-spin operator, $\boldsymbol{g}$ is the g tensor of electron spins, $\boldsymbol{B}$ is the external static magnetic field, $\boldsymbol{D}$ is the fine structure tensor, and D and E are the zfs parameters.[12,13] In order to reduce the computing time, the resonance magnetic fields ($B_{M_s \Leftrightarrow M_s+1}$) and the transition probabilities ($TP_{M_s \Leftrightarrow M_s+1}$) for single transitions between the M_s and $M_s + 1$ sublevels of the quartet state were calculated using the perturbation theory.[13] The calculated equations were applicable to our system, since $\nu \sim 10$ GHz and $D < 0.3$ GHz.

For the excited triplet spectra, the ESP is produced by selectivity of the ISC from the excited singlet state to each excited triplet sublevel. Because the SOC between the excited singlet state and the excited triplet eigenfunctions in zero magnetic field is important for the ISC, the eigenfunctions in the resonance magnetic field must be expressed by a linear combination of the eigenfunctions in zero magnetic field. Therefore, it is necessary for the calculation of the excited quartet ESP to obtain the eigenfunctions in the resonance magnetic field, which are expressed by a linear combination of the eigenfunctions in zero magnetic field. A 4×4 matrix in Chart 1 was diagonalized to obtain the eigenfunctions ($|Q,M_s\rangle$; $M_s = -^3/_2, -^1/_2, {}^1/_2$, and $^3/_2$) in the resonance magnetic fields.[14] The eigenfunction, $|Q,M_s\rangle$, was expressed by a linear combination of the basic functions, $|Q,M_s'\rangle$, which were eigenfunctions when $B_{M_s \Leftrightarrow M_s+1} = E = 0$, such as[15]

$$|Q,M_s\rangle = \sum_{M_s'} C_{M_s,M_s'} |Q,M_s'\rangle \quad (2)$$

For the excited triplet state, the population of each eigenstate in the resonance magnetic field is determined by both the magnitude of the SOC between the excited singlet state and the triplet eigenfunctions in zero magnetic field and the square of the coefficients of each basic function. Since the SOC between the excited doublet state and each $|Q,M_s'\rangle$ might also be efficient for the ESP, the population of the $|Q,M_s\rangle$ state, P_{M_s}, was calculated using the magnitude of the SOC between the excited doublet and $|Q,M_s'\rangle$ states, $P_{M_s'}$, as follows:[15]

(11) Fujisawa, J.; Ishii, K.; Ohba, Y.; Yamauchi, S. *J. Phys. Chem. A* **1997**, *101*, 5869.

(12) The g anisotropy was not considered in the simulation.

(13) Teki, Y.; Takui, T.; Itoh, K. *J. Chem. Phys.* **1988**, *88*, 6134.

(14) (a) Reibisch, K.; Kothe, H.; Brickmann, J. *Chem. Phys. Lett.* **1972**, *17*, 86. (b) Brickmann, J.; Kothe, G. *J. Chem. Phys.* **1973**, *59*, 2807.

(15) When $E \neq 0$, the eigenfunctions and populations in zero magnetic field were rewritten using $|Q,M_s'\rangle$ and $P_{M_s'}$ as follows: $|Q,\pm^3/_2''\rangle = \cos\omega|Q,\pm^3/_2'\rangle + \sin\omega|Q,\mp^1/_2'\rangle$. $|Q,\pm^1/_2''\rangle = \cos\omega|Q,\pm^1/_2'\rangle - \sin\omega|Q,\mp^3/_2'\rangle$. $P_{\pm3/2''} = \cos^2\omega P_{\pm3/2'} + \sin^2\omega P_{\mp1/2'}$. $P_{\pm1/2''} = \cos^2\omega P_{\pm1/2'} + \sin^2\omega P_{\mp3/2'}$. $\tan 2\omega = \sqrt{3}E/D$.

$$P_{M_s} = \sum_{M_s'} C_{M_s,M_s'}{}^2 P_{M_s'} \quad (3)$$

The ESP of the transition between the $|Q,M_s\rangle$ and $|Q,M_s+1\rangle$ sublevels, $P_{M_s \leftrightarrow M_s+1}$, was represented as

$$P_{M_s \leftrightarrow M_s+1} = P_{M_s} - P_{M_s+1} \quad (4)$$

When the population of the upper sublevel, P_{M_s+1}, is larger than that of the lower sublevel, P_{M_s}, the $P_{M_s \leftrightarrow M_s+1}$ is negative and exhibits an emission of microwave. In contrast, when $P_{M_s+1} < P_{M_s}$, the $P_{M_s \leftrightarrow M_s+1}$ is positive and shows an absorption of microwave.

As a result, the line-shape function, $h(B)$, was expressed using $B_{M_s \leftrightarrow M_s+1}$, $TP_{M_s \leftrightarrow M_s+1}$, and $P_{M_s \leftrightarrow M_s+1}$ as follows:

$$h(B) = \sum_{M_s} \int_0^{2\pi} d\varphi \int_0^{\pi} d\phi \int_0^{\pi/2} d\theta \sin\theta \, TP_{M_s \leftrightarrow M_s+1} \times P_{M_s \leftrightarrow M_s+1} \times f(B - B_{M_s \leftrightarrow M_s+1}) \quad (5)$$

Here, $f(B - B_{M_s \leftrightarrow M_s+1})$ is the line-shape function for a single transition, for which the Gaussian line-shape function was employed.

Results and Interpretations

1. Absorption and Phosphorescence Spectra. The absorption spectra of ZnTPP and *p*-nitpy in toluene are shown in Figure 2. The absorption spectrum of *m*-nitpy is almost identical with that of *p*-nitpy. From the absorption spectrum, the lowest excited singlet state of ZnTPP (^{1}ZnTPP*) is at 1.7×10^4 cm^{-1}. The lowest excited doublet state of *p*- or *m*-nitpy (^{2}nitpy*) is estimated as 1.4×10^4 cm^{-1}. The phosphorescence spectrum of ZnTPP−*p*-nitpy at 77 K is also shown in Figure 2.[16] Since the phosphorescence maximum is detected at 793 nm, the energies of the lowest excited doublet (D_1) and the lowest excited quartet (Q_1) states, which are constituted by the lowest excited triplet state of ZnTPP (^{3}ZnTPP*) and the doublet ground state of nitpy (^{2}nitpy), are estimated as 1.3×10^4 cm^{-1}.

2. TREPR Spectra. TREPR spectra of ZnTPP−*p*-nitpy and ZnTPP−*m*-nitpy observed at 0.5 μs and 20 K are shown in Figure 3. Two kinds of signals due to ZnTPP−*p*-nitpy were observed. One is a pair of signals giving an *A/E* polarization pattern, which shows an absorption (*A*) and an emission (*E*) of the microwave at the lower magnetic field (307 mT) and higher magnetic field (342 mT) sides, respectively. The other is a relatively sharp signal with *E* polarization at $g = 1.999 \pm 0.002$. For ZnTPP−*m*-nitpy, two kinds of signals were also observed. One is a pair of signals giving the *A/E* pattern, which is the same polarization pattern of the para complex, but has different resonance magnetic fields at 308 and 340 mT. The other is a sharp signal with *A* polarization at $g = 2.002 \pm 0.001$, contrary to the para complex.

The time profiles of the TREPR signals for both the para and meta complexes are shown in Figure 4. For the para complex, the time profile of the *A* signal at low magnetic field (dotted line) is similar to that of the *E* signal at high magnetic field (broken line), as shown in Figure 4a. The time profile of the signal around $g = 2.00$ (solid line) is constituted by both a fast component with *E* polarization and a slow component with *A* polarization and is obviously different from those of the *A/E* signals. The time profiles of the meta complex are shown in Figure 4b. By analogy with the para complex, the time profile of the *A* signal at low magnetic field (dotted line) is identical with that of the *E* signal at high magnetic field (broken line). The time profile of the signal at $g = 2.00$ (solid line) contains two components, a fast *A* component and a slow *A* component, and differs from those of the *A/E* signals.

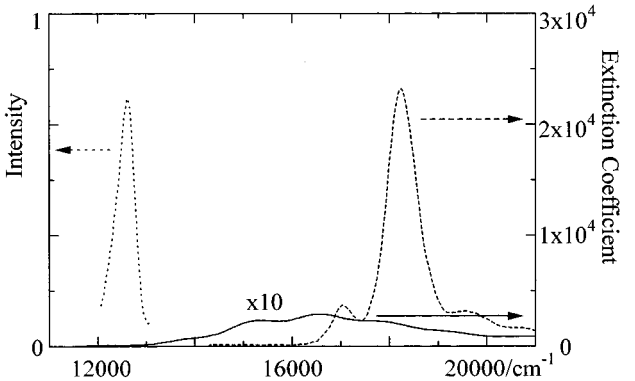

Figure 2. Absorption spectra of ZnTPP (broken line) and *p*-nitpy (solid line) and a phosphorescence spectrum of ZnTPP−*p*-nitpy (dotted line).

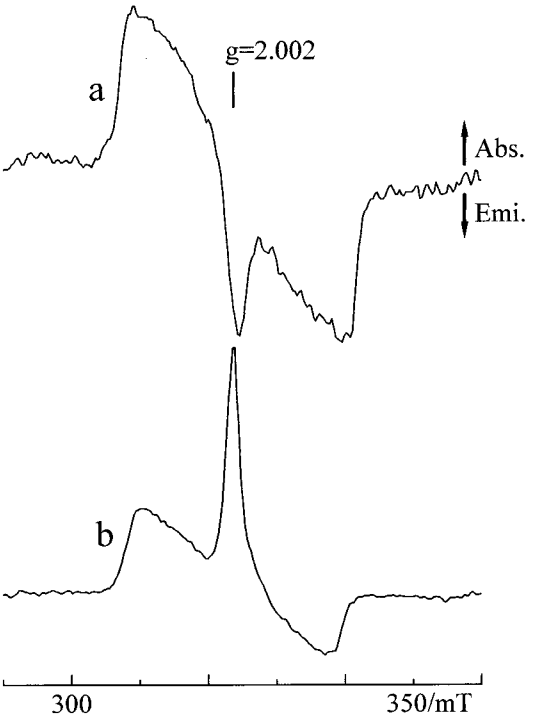

Figure 3. TREPR spectra of (a) ZnTPP−*p*-nitpy and (b) ZnTPP−*m*-nitpy. All spectra were observed at 20 K and 0.5 μs after laser excitation.

Spectral simulations of the excited quartet state with ESP were carried out for both the para and meta complexes, as shown in Figures 5 and 6.[17] Although the obtained TREPR spectra are constituted by the *A/E* signals and the sharp signal at $g = 2.00$, the spectra were simulated to fit the *A/E* signals. As revealed, the *A/E* signals were reproduced very well by the simulation. On the other hand, the simulation spectra fitted in the region around $g = 2.00$ are shown in Figure 7. The spectra were calculated for $P_{+3/2'}:P_{+1/2'}:P_{-1/2'}:P_{-3/2'} = 0:1:2:1$ and $P_{+3/2'}:P_{+1/2'}:P_{-1/2'}:P_{-3/2'} = 1:2:1:0$.[18] When the simulation spectra have a peak around $g = 2.00$, the absorptive pattern at low magnetic field is distinct from the emissive pattern at high magnetic field. These simulation spectra are unlike the TREPR

(16) The phosphorescence decays at 80 K were reproduced by a sum of two exponential decays for both the para and the meta complexes. The two lifetimes were 0.38/4 and 0.27/0.8 ms for the para and meta complexes, respectively.

(17) When $P_{+3/2''}:P_{+1/2''}:P_{-1/2''}:P_{-3/2''} = 0:1:1:0$, the simulation spectra were the same as those in Figures 5 and 6.

(18) When $P_{+3/2''}:P_{+1/2''}:P_{-1/2''}:P_{-3/2''} = 0:1:2:1$ and $P_{+3/2''}:P_{+1/2''}:P_{-1/2''}:P_{-3/2''} = 1:2:1:0$, the simulation spectra were the same as those in Figures 7a and 7b, respectively.

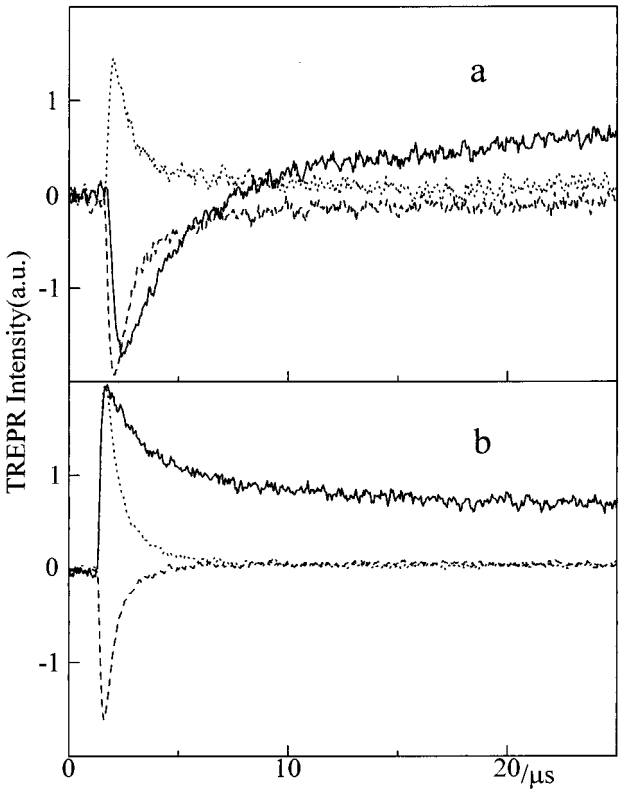

Figure 4. Time profiles of (a) ZnTPP−*p*-nitpy and (b) ZnTPP−*m*-nitpy observed at 20 K. Dotted lines, broken lines, and solid lines denote the *A* signal at low magnetic field, the *E* signal at high magnetic field, and the sharp signal at $g = 2.00$, respectively.

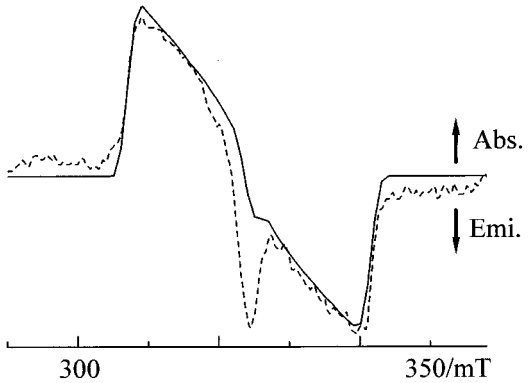

Figure 5. TREPR spectrum of ZnTPP−*p*-nitpy (broken line) with its simulation (solid line). Simulation parameters were summarized in Table 1.

spectra observed for the ZnTPP−nitpy systems. It is reliable to simulate the *A/E* signals from the fact that the *A/E* signals are evidently assigned to transitions between the $|Q_1,\pm^3/_2\rangle$ and $|Q_1,\pm^1/_2\rangle$ sublevels, judging from the magnitude of the splitting.[10] Further, it was supported to separate the sharp signal at $g = 2.00$ from the *A/E* signals by the fact that the time profile of the signal at $g = 2.00$ was obviously different from those of the *A/E* signals. The parameters used for the simulations in Figures 5 and 6 are summarized in Table 1. The *D* value (0.22 GHz) of the meta complex was a little smaller than that (0.24 GHz) of the para complex. The populations of $|Q_1,\pm^1/_2'\rangle$, $P_{\pm 1/2'}$, were larger than those of $|Q_1,\pm^3/_2'\rangle$, $P_{\pm 3/2'}$, for both the para and the meta complexes.

The sharp peaks at $g = 2.00$ and 0.5 μs could not be simulated as the excited quartet state for both the para and the meta complexes. From the peak in the solid state ($g = 2.007$ and

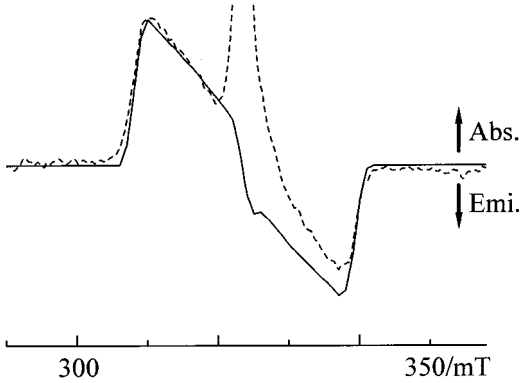

Figure 6. TREPR spectrum of ZnTPP−*m*-nitpy (broken line) with its simulation (solid line). Simulation parameters were summarized in Table 1.

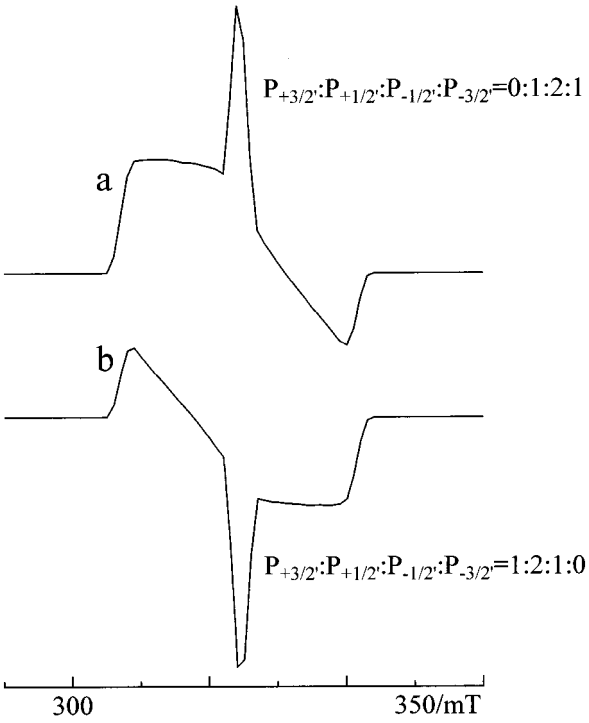

Figure 7. Excited quartet spectra calculated for (a) $P_{+3/2'}:P_{+1/2'}:P_{-1/2'}:P_{-3/2'} = 0:1:2:1$ and for (b) $P_{+3/2'}:P_{+1/2'}:P_{-1/2'}:P_{-3/2'} = 1:2:1:0$. All spectra were calculated using $D = 0.24$ GHz and $E = 0.08$ GHz.

Table 1. Zfs Parameters and ISC Ratio

complex	$D(Q_1)$/ GHz[a]	$E(Q_1)$/ GHz[a]	$P_{3/2'}:P_{1/2'}:P_{-1/2'}:P_{-3/2'}$[a]	$D_{calc}(Q_1)$/ GHz[b]
ZnTPP−*p*-nitpy	0.24	0.08	0:1:1:0	0.233
ZnTPP−*m*-nitpy	0.22	0.07	0:1:1:0	0.224

[a] The parameters used for the simulation. See the text. [b] The $D_{calc}(Q_1)$ values were calculated using a point−charge approximation. See the text.

2.006 for the para and meta complexes, respectively), the doublet ground state was easily eliminated from the candidates for these peaks.[19] Consequently, these sharp peaks are assigned to the lowest excited doublet (D_1) state.[20,21] The ESPs of the D_1 state were the *E* and *A* polarizations for the para and meta complexes,

(19) Since the *J* value is not variable in the solid state, the ESP of the D_0 state due to the radical−triplet pair mechanism cannot occur, unlike in solution.

(20) For Cu porphyrins, the lifetime of the D_1 state was estimated as ~70 μs in the solid state.[21] Therefore, the D_1 state in the ZnTPP−nitpy systems, where the interaction between the doublet and triplet spins was weaker than that in Cu porphyrins, was observable by TREPR.

Table 2. *g* Values

complex	$g(D_1)^a$	$g(Q_1)^a$	$g_{calc}(D_1)^b$	$g_{calc}(Q_1)^b$
ZnTPP−*p*-nitpy	1.999	2.004	1.995 (2.000)	2.001 (2.004)
ZnTPP−*m*-nitpy	2.002	2.002	1.995 (2.001)	2.000 (2.003)

[a] The *g* values were evaluated from the TREPR spectra. [b] The *g* values were calculated using the $g(T_1)$ and the $g(R)$ values obtained from the experiments. The *g* values in parentheses were calculated using $g(T_1) = 2.002$.

respectively. It was found from the polarization that the populations of the D_1 state for the para and meta complexes were distributed selectively in the $|D_1,+^1/_2\rangle$ and $|D_1,-^1/_2\rangle$ sublevels, respectively.

According to our communication,[10] the slow component at $g = 2.00$ with the *A* polarization is assigned to the excited quartet state under the Boltzmann distribution for both the para and the meta complexes.[22] The observed *g* values of the D_1 state, $g(D_1)$, are 1.999 and 2.002 for the para and meta complexes, respectively. The observed *g* values of the Q_1 state, $g(Q_1)$, are 2.004 ± 0.001 and 2.002 ± 0.001 for the para and meta complexes, respectively. These *g* values are summarized in Table 2.

Discussion

1. Wavefunctions of the Excited Doublet and Quartet States Constituted by ^{1,3}ZnTPP and ^{2}nitpy. To clarify the electronic properties, spin−orbit functions are investigated. From the absorption spectrum, ^{1}ZnTPP* is at 1.7×10^4 cm^{-1}. In the lowest excited singlet region, $^1E_{u_x}$ and $^1E_{u_y}$ states are degenerate. The $^1E_{u_y}$ ($^1E_{u_x}$) state is constituted by two electronic configurations, $^1(a_{1u}e_{g_x})$ and $^1(a_{2u}e_{g_y})$ (or $^1(a_{1u}e_{g_y})$ and $^1(a_{2u}e_{g_x})$).[23] a_{2u} and a_{1u} denote the highest occupied molecular orbital (HOMO) and the second HOMO, respectively. e_{g_x} and e_{g_y} are the lowest unoccupied MO (LUMO). Therefore, the wavefunctions of $^2(^1$ZnTPP*−^{2}nitpy), i.e., the D_4 and D_5 states, are expressed as follows:[21]

$$|D_4,+^1/_2'\rangle = (|a_{1u}\bar{e}_{g_y}a_{2u}\bar{a}_{2u}r| - |\bar{a}_{1u}e_{g_y}a_{2u}\bar{a}_{2u}r| - |a_{1u}\bar{a}_{1u}a_{2u}\bar{e}_{g_x}r| + |a_{1u}\bar{a}_{1u}\bar{a}_{2u}e_{g_x}r|)/2 \quad (6a)$$

$$|D_4,-^1/_2'\rangle = (|a_{1u}\bar{e}_{g_y}a_{2u}\bar{a}_{2u}\bar{r}| - |\bar{a}_{1u}e_{g_y}a_{2u}\bar{a}_{2u}\bar{r}| - |a_{1u}\bar{a}_{1u}a_{2u}\bar{e}_{g_x}\bar{r}| + |a_{1u}\bar{a}_{1u}\bar{a}_{2u}e_{g_x}\bar{r}|)/2 \quad (6b)$$

$$|D_5,+^1/_2'\rangle = (|a_{1u}\bar{e}_{g_x}a_{2u}\bar{a}_{2u}r| - |\bar{a}_{1u}e_{g_x}a_{2u}\bar{a}_{2u}r| - |a_{1u}\bar{a}_{1u}a_{2u}\bar{e}_{g_y}r| + |a_{1u}\bar{a}_{1u}\bar{a}_{2u}e_{g_y}r|)/2 \quad (6c)$$

$$|D_5,-^1/_2'\rangle = (|a_{1u}\bar{e}_{g_x}a_{2u}\bar{a}_{2u}\bar{r}| - |\bar{a}_{1u}e_{g_x}a_{2u}\bar{a}_{2u}\bar{r}| - |a_{1u}\bar{a}_{1u}a_{2u}\bar{e}_{g_y}\bar{r}| + |a_{1u}\bar{a}_{1u}\bar{a}_{2u}e_{g_y}\bar{r}|)/2 \quad (6d)$$

Here, r denotes the singly occupied MO (SOMO) of nitpy. The coefficient of $^1(a_{1u}e_{g_x})$ is assumed to be equal to that of $^1(a_{2u}e_{g_y})$.[23] On the other hand, the wavefunctions of $^2(^1$ZnTPP−^{2}nitpy*), which are located at 1.4×10^4 cm^{-1}, are[21]

$$|D_3,+^1/_2'\rangle = |a_{1u}\bar{a}_{1u}a_{2u}\bar{a}_{2u}d| \quad (7a)$$

$$|D_3,-^1/_2'\rangle = |a_{1u}\bar{a}_{1u}a_{2u}\bar{a}_{2u}\bar{d}| \quad (7b)$$

Here, d denotes the highest doubly occupied MO of nitpy.

The energy of ZnTPP coordinated by pyridine in the lowest excited triplet state, ^{3}ZnTPP*−py, was estimated as 1.3×10^4 cm^{-1} from the phosphorescence spectrum.[24] In the lowest excited triplet region, $^3E_{u_x}$ and $^3E_{u_y}$ states are degenerate similarly to the $^1E_{u_x}$ and $^1E_{u_y}$ states but are single electronic configurations with little configuration interaction. ^{3}ZnTPP* is known to be a pure $^3(a_{2u}e_g)$ configuration.[7,25] Therefore, the wavefunctions of $^{2,4}(^3$ZnTPP*−^{2}nitpy) are represented as follows:[21]

$$|D_1,+^1/_2'\rangle = (2|a_{1u}\bar{a}_{1u}a_{2u}e_{g_x}\bar{r}| - |a_{1u}\bar{a}_{1u}a_{2u}\bar{e}_{g_x}r| - |a_{1u}\bar{a}_{1u}\bar{a}_{2u}e_{g_x}r|)/\sqrt{6} \quad (8a)$$

$$|D_1,-^1/_2'\rangle = (-2|a_{1u}\bar{a}_{1u}\bar{a}_{2u}\bar{e}_{g_x}r| + |a_{1u}\bar{a}_{1u}\bar{a}_{2u}e_{g_x}\bar{r}| + |a_{1u}\bar{a}_{1u}a_{2u}\bar{e}_{g_x}\bar{r}|)/\sqrt{6} \quad (8b)$$

$$|Q_1,+^3/_2'\rangle = |a_{1u}\bar{a}_{1u}a_{2u}e_{g_x}r| \quad (9a)$$

$$|Q_1,+^1/_2'\rangle = (|a_{1u}\bar{a}_{1u}\bar{a}_{2u}e_{g_x}r| + |a_{1u}\bar{a}_{1u}a_{2u}\bar{e}_{g_x}r| + |a_{1u}\bar{a}_{1u}a_{2u}e_{g_x}\bar{r}|)/\sqrt{3} \quad (9b)$$

$$|Q_1,-^1/_2'\rangle = (|a_{1u}\bar{a}_{1u}a_{2u}\bar{e}_{g_x}\bar{r}| + |a_{1u}\bar{a}_{1u}\bar{a}_{2u}e_{g_x}\bar{r}| + |a_{1u}\bar{a}_{1u}\bar{a}_{2u}\bar{e}_{g_x}r|)/\sqrt{3} \quad (9c)$$

$$|Q_1,-^3/_2'\rangle = |a_{1u}\bar{a}_{1u}\bar{a}_{2u}\bar{e}_{g_x}\bar{r}| \quad (9d)$$

The wavefunctions of the D_2 and Q_2 states are the same as eqs 8 and 9 with an exchange between the e_{g_y} and e_{g_x} orbitals.

2. Obtained EPR Parameters. The *D* value of the meta complex was a little smaller than that of the para complex. To clarify this origin, the $D(Q_1)$ values were calculated by diagonalizing the following tensor:[10,26]

$$\boldsymbol{D}(Q_1) = \{\boldsymbol{D}(T_1) + \boldsymbol{D}(RT_1)\}/3 \quad (10)$$

Here, $\boldsymbol{D}(Q_1)$, $\boldsymbol{D}(T_1)$, and $\boldsymbol{D}(RT_1)$ are the zfs tensors for the excited quartet, the excited triplet, and the magnetic dipolar−dipolar interaction between the excited triplet and the radical, respectively. $\boldsymbol{D}(T_1)$ was obtained from the measurement of ^{3}ZnTPP*−py. $\boldsymbol{D}(RT_1)$ were calculated under a point−charge approximation.[10,27] The calculation results are summarized in Table 1. The calculated $D(Q_1)$ (0.224 GHz) of the meta complex was a little smaller than that (0.233 GHz) of the para complex. This order is consistent with the experimental results and is explained by the fact that the $D(RT_1)$ of the meta complex is negatively larger than that of the para complex, because the

(21) (a) Eastwood, D.; Gouterman, M. *J. Mol. Spectrosc.* **1969**, *30*, 437. (b) Ake, R. L.; Gouterman, M. *Theoret. Chim. Acta* **1969**, *15*, 20. (c) Gouterman, M.; Mathies, R. A.; Smith, B. E.; Caughey, W. S. *J. Chem. Phys.* **1970**, *52*, 3795. (d) Gouterman, M. In *The Porphyrins*; Dolphin, D., Ed.; Academic: New York, 1978; Vol. III, pp 1−165.

(22) The Q_1 state under the Boltzmann distribution was observable for the lifetime of the phosphorescence.[16]

(23) (a) Gouterman, M. *J. Chem. Phys.* **1959**, *30*, 1139. (b) Gouterman, M. *J. Mol. Spectrosc.* **1961**, *6*, 138. (c) Gouterman, M.; Wagniere, G. H.; Snyder, L. C. *J. Mol. Spectrosc.* **1963**, *11*, 108. (d) Weiss, C.; Kobayashi, H.; Gouterman, M. *J. Mol. Spectrosc.* **1965**, *16*, 415.

(24) Walters, V. A.; Phillips, C. M. *J. Phys. Chem.* **1995**, *99*, 1166.

(25) Langnoff, S. R.; Davidson, E. R.; Gouterman, M.; Leenstra, W. R.; Kwiram, A. L. *J. Chem. Phys.* **1975**, *62*, 169.

(26) Bencini, A.; Gatteschi, D. *EPR of Exchange Coupled Systems*; Springer-Verlag: Berlin, 1990.

(27) (a) Stewart, J. J. P. *J. Comp. Chem.* **1989**, *10*, 209. (b) Awaga, K.; Inabe, T.; Maruyama, Y. *Chem. Phys. Lett.* **1992**, *190*, 349. (c) Collins, D. M.; Hoard, J. L. *J. Am. Chem. Soc.* **1970**, *92*, 3761. (d) Sekino, H.; Kobayashi, H. *J. Chem. Phys.* **1987**, *86*, 5045.

distance between the radical center and ^{3}ZnTPP* for the meta complex is smaller than that for the para complex.

The $g(D_1)$ and $g(Q_1)$ values are represented theoretically as follows:

$$g(D_1) = \{-g(R) + 4g(T_1)\}/3 \quad (11)$$

$$g(Q_1) = \{g(R) + 2g(T_1)\}/3 \quad (12)$$

From the peaks in the solid state, the $g(R)$ values were estimated as 2.007 ± 0.001 and 2.006 ± 0.001 for *p*- and *m*-nitpy, respectively. $g(T_1)$ was evaluated as 1.998 ± 0.003 for ^{3}ZnTPP*−py. Using these values, $g(D_1)$ and $g(Q_1)$ were calculated theoretically, as summarized in Table 2. All the *g* values calculated are smaller than those obtained experimentally. These differences are considered to be due to the small $g(T_1)$ value. The smaller $g(T_1)$ value (=1.998) of ^{3}ZnTPP*−py compared with the free-electron value (=2.0023) is interpreted by Zeeman interaction and the SOC between the T_1 and T_2 states.[7d,28] The interaction between the T_1 and T_2 states would be decreased by the coordination of *p*- or *m*-nitpy, which provides interaction between the SOMO of nitpy and the LUMO of ZnTPP. As a result, the $g(T_1)$ value of the ZnTPP−nitpy system could be close to the free-electron value. The $g(D_1)$ and $g(Q_1)$ values calculated using $g(T_1) = 2.002$ are in good agreement with those observed, as summarized in Table 2.

3. Electron-Spin Polarization in the Excited Quartet State. It was found from the simulation results that the excited quartet spectra of ZnTPP−*p*-nitpy and ZnTPP−*m*-nitpy were explained by selective ISC from the excited doublet states to the $|Q_1,\pm^1/_2'\rangle$ spin sublevels. To clarify the origin, we calculated the SOC between some excited doublet and Q_1 states. Since the ESP of ^{3}ZnTPP* was reasonably interpreted by the SOC due to the d_π atomic orbitals on the heavy zinc ion,[7,21b,29] the SOC due to the zinc ion between the excited doublet and Q_1 states is considered. The SOC between the D_3 and Q_1 states, ^{2}(^{1}ZnTPP−^{2}nitpy*) and ^{4}(^{3}ZnTPP*−^{2}nitpy), is easily neglected, since the SOC hamiltonian, H_{SO}, is a one-electron operator. In contrast, the matrix elements of the SOC between the D_5 and Q_1 states were calculated using eqs 6 and 9 as follows:[7d,21]

$$\langle D_5,I'|H_{SO}|Q_1,K'\rangle = iZ/2\sqrt{3} \qquad (I = K)$$

$$\langle D_5,I'|H_{SO}|Q_1,K'\rangle = 0 \qquad (I \neq K) \quad (13)$$

$$iZ = \eta^2\langle d_{yz}|\xi l_z|d_{xz}\rangle$$

Here, *Z* is a matrix element of the SOC.[7d] η is the e_g MO coefficient of the d_{xz} (d_{yz}) orbital on the zinc ion.[7d] It was indicated that the ISC to $|Q_1,\pm^1/_2'\rangle$ was selective. These calculation results are consistent with the experimental results.

Next the SOC between the D_2 and Q_1 states is considered. The matrix elements were calculated as follows.[21]

$$\langle D_2,I'|H_{SO}|Q_1,K'\rangle = iZ/3\sqrt{2} \qquad (I = K)$$

$$\langle D_2,I'|H_{SO}|Q_1,K'\rangle = 0 \qquad (I \neq K) \quad (14)$$

The selectivity of the SOC between the D_2 and Q_1 states is the same as that between the D_5 and Q_1 states and is consistent with the experimental results. On the other hand, the spin−orbit interactions between the D_4 and Q_1 states and between the D_1 and Q_1 states were neglected, because the e_{g_x} MO coefficient of the d_{yz} orbital was negligible.[7d] Consequently, the selective ISC to the $|Q_1,\pm^1/_2'\rangle$ is reasonably interpreted by the SOC between the D_5 and Q_1 states or between the D_2 and Q_1 states.

4. Electron-Spin Polarization in the Excited Doublet State. The TREPR spectra of ^{2}(^{3}ZnTPP*−^{2}nitpy) showed *E* and *A* polarizations for the para and meta complexes, respectively. It was found from the polarization that the populations of the D_1 state were distributed selectively in the $|D_1,+^1/_2\rangle$ and $|D_1,-^1/_2\rangle$ sublevels for the para and meta complexes, respectively. The electron-spin-polarization mechanisms of the doublet state reported previously are divided into two groups. In one case, the ESP is generated from the change in the magnitude of the exchange interaction, *J*, such as a radical pair mechanism,[3] and a radical−triplet pair mechanism (RTPM).[30−32] In the second case, the ESP is induced by the SOC, such as a triplet mechanism,[2] and an electron-spin polarization-transfer mechanism (ESPT).[33] In our system, the molecular dynamics can be neglected, since the molecules at 20 K were in the rigid solid state. Further, the triplet exciton is slow in the glassy matrix, unlike in a crystal.[31] Because the *J* value is not variable in our system, the ESP due to the RTPM can be neglected. Further, the ESPT from the Q_1 molecule to the D_1 molecule cannot occur without both the molecular dynamics and the exciton. It is therefore considered as the other candidate of our ESPs that the polarization originates from the fact that the internal conversion rate from the higher excited doublet states to $|D_1,+^1/_2\rangle$ is different from that to $|D_1,-^1/_2\rangle$. The perturbation between the D_1 and Q_1 states is considered as one of the origins, since the contribution of the Q_1 state to the D_1 state would interfere with the internal conversion between the excited doublet states in analogy with radical pairs.[4,5] The Q_1 state of the radical−triplet pair can perturb the nearby D_1 state a little, because of the small energy difference between the D_1 and Q_1 states. Since the energy difference between the $g(R)\beta B$ and $g(T_1)\beta B$ values is smaller than the zfs energy in the solid state, only the zfs interaction, H_{zfs}, between the D_1 and Q_1 states is considered.[31] The wavefunctions of the excited doublet state, $|D_1,I^{\pm}\rangle$, are represented as follows:

$$|D_1,I^{\pm}\rangle = N_I\{|D_1,I\rangle + \sum_K (H_{I,K}/\Delta E_{I,K})|Q_1,K\rangle\} \quad (15a)$$

$$H_{I,K} = \langle Q_1,K|H_{zfs}|D_1,I\rangle \quad (15b)$$

$$\Delta E_{I,K} = 3J - \langle Q_1,K|H_{spin}|Q_1,K\rangle + \langle D_1,I|H_{spin}|D_1,I\rangle \quad (15c)$$

Here, N_I is a normalization constant and exhibits a coefficient of $|D_1,I\rangle$. The zfs interactions between the D_1 and Q_1 states for $B||z$ are shown in Figure 8. When $J < 0$, the interaction between $|D_1,+^1/_2\rangle$ and $|Q_1,-^3/_2\rangle$ is larger than that between

(28) Kooter, J. A.; Canters, G. W.; van der Waals, J. H. *Mol. Phys.* **1977**, *33*, 1545.

(29) van Dorp, W. G.; Schoemaker, W. H.; Soma, M.; van der Waals, J. H. *Mol. Phys.* **1975**, *30*, 1701.

(30) (a) Blättler, C.; Jent, F.; Paul, H. *Chem. Phys. Lett.* **1990**, *166*, 375. (b) Kawai, A.; Okutsu, T.; Obi, K. *J. Phys. Chem.* **1991**, *95*, 9130. (c) Kawai, A.; Obi, K. *J. Phys. Chem.* **1992**, *96*, 52. (d) Kawai, A.; Obi, K. *Res. Chem. Intermed.* **1993**, *19*, 865. (e) Turro, N. J.; Khudyakov, I. V.; Bossmann, S. H.; Dwyer, D. W. *J. Phys. Chem.* **1993**, *97*, 1138.

(31) (a) Corvaja, C.; Franco, L.; Pasimeni, L.; Toffoletti, A.; Montanari, L. *Chem. Phys. Lett.* **1993**, *210*, 355. (b) Corvaja, C.; Franco, L.; Toffoletti, A. *Appl. Magn. Reson.* **1994**, *7*, 257. (c) Corvaja, C.; Franco, L.; Pasimeni, L.; Toffoletti, A. *J. Chem. Soc., Faraday Trans.* **1994**, *90*, 3267.

(32) (a) Hugerat, M.; van der Est, A.; Ojadi, E.; Biczok, L.; Linschitz, H.; Levanon, H.; Stehlik, D. *J. Phys. Chem.* **1996**, *100*, 495. (a) Regev. A.; Galili, T.; Levanon, H. *J. Phys. Chem.* **1996**, *100*, 18502.

(33) (a) Fujisawa, J.; Ishii, K.; Ohba, Y.; Iwaizumi, M.; Yamauchi, S. *J. Phys. Chem.* **1995**, *99*, 17082. (b) Jenks, W. S.; Turro, N. J. *Res. Chem. Intermed.* **1990**, *13*, 237.

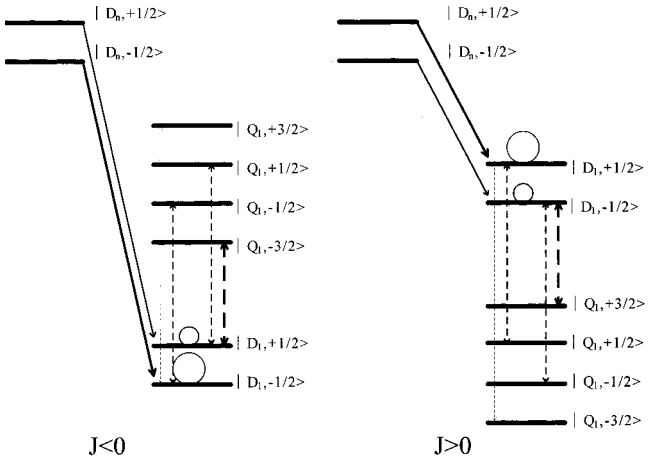

Figure 8. Perturbation between the D_1 and Q_1 states. Arrows constituted by solid lines show internal conversion routes. Arrows constituted by broken lines represent the magnitude of the interaction between the D_1 and Q_1 states.

$|D_1,-^1/_2\rangle$ and $|Q_1,+^3/_2\rangle$ due to the energy difference. Therefore, the contribution of the Q_1 state to $|D_1,+^1/_2{}^{\ddagger}\rangle$, $1 - N_{+1/2}{}^2$, which provides the interfering factor of internal conversion, is larger than that to $|D_1,-^1/_2{}^{\ddagger}\rangle$, $1 - N_{-1/2}{}^2$. By this perturbation, the internal conversion rate to $|D_1,+^1/_2{}^{\ddagger}\rangle$ is considered to be slower than that to $|D_1,-^1/_2{}^{\ddagger}\rangle$. This difference results in the *A* polarization. In contrast, the internal conversion rate to $|D_1,+^1/_2{}^{\ddagger}\rangle$ is considered to be faster than that to $|D_1,-^1/_2{}^{\ddagger}\rangle$, when $J > 0$. This provides the *E* polarization. From the RTPM experiments at room temperature,[11] the signs of the *J* values were determined as positive and negative for the para and meta complexes, respectively. The determined *J* signs were reasonably explained by their molecular orbital overlaps.[11] According to Figure 8, the *E* and *A* polarizations are provided using the *J* signs for the para and meta complexes, respectively, and are consistent with the observation. This fact supports our polarization mechanism.[34,35] Although it was difficult to resolve the structural anisotropy in contrast to the excited quartet state, this mechanism is proposed to be a candidate for the ESPs in the D_1 state.

(34) To discuss quantitatively, the contributions of the excited quartet configurations, $1 - N_I{}^2$, were calculated. For example, when $3J = 1$ cm^{-1} and $\boldsymbol{B}||z$, $1 - N_I{}^2$ were calculated as 2.7×10^{-4} and 6.8×10^{-4} for $I = ^1/_2$ and $-^1/_2$, respectively. Here, we used $B = 330$ mT, $D(T_1) = 0.912$ GHz, $D(RT_1) = -0.214$ GHz, $E(T_1) = 0.284$ GHz, and $E(RT_1) = 0$ GHz. The obtained $1 - N_{+1/2}{}^2$ is a little smaller than $1 - N_{-1/2}{}^2$. Since the total population of the D_1 state is large from spin multiplicity, the difference between the population of $|D_1,+^1/_2{}^{\ddagger}\rangle$, $P_{D,+1/2^{\ddagger}}$, and that of $|D_1,-^1/_2{}^{\ddagger}\rangle$, $P_{D,-1/2^{\ddagger}}$, would be large enough to observe.

(35) Although the *J* value of the meta complex differed from that of the para complex in both the sign and the magnitude, the observed spectrum of the meta complex was almost the same as that of the para complex except for the sharp signal around $g = 2.00$. From these results, it was concluded that the polarization due to the zfs interaction was not observed in the excited quartet spectra. This is reasonable, since both the contribution of the D_1 state to the Q_1 state and the difference between $P_{D,+1/2^{\ddagger}}/(P_{D,+1/2^{\ddagger}} + P_{D,-1/2^{\ddagger}})$ and $P_{D,-1/2^{\ddagger}}/(P_{D,+1/2^{\ddagger}} + P_{D,-1/2^{\ddagger}})$ are small.

Conclusions and Outlook

In this report, we have studied the excited states of the paramagnetic complexes, ZnTPP−*p*-nitpy and ZnTPP−*m*-nitpy, by the TREPR method. The obtained TREPR spectra were reasonably assigned using the *g* and *D* values, and the excited quartet EPR spectra with ESP were simulated accurately for the first time. From the spectral simulations, it was established in general that ESP in the excited quartet state was interpreted by selective ISC, which was produced by SOC between the excited doublet states and the eigenfunctions of the quartet state in zero magnetic field. The TREPR spectra of the ZnTPP−nitpy systems were interpreted by selective ISC to the $|Q_1,\pm^1/_2{}'\rangle$ sublevels. This selectivity originated from the SOC due to the zinc ion between the D_2 and Q_1 states or between the D_5 and Q_1 states. The ESP in the D_1 state was interpreted by the difference between the internal conversion rate to $|D_1,+^1/_2\rangle$ and that to $|D_1,-^1/_2\rangle$.

From this study, various kinds of developments are predicted, as follows. Firstly, the excited multiplet states, which have higher spin multiplicities, will be observed and characterized. Secondly, the application of the TREPR to paramagnetic metallo complexes is recommended. The magnetic properties of paramagnetic metallo complexes in the excited state are important not only for the investigation of the excited state but also for the analysis of the magnetic properties in the ground state. In addition, studies on the interaction between an excited triplet molecule and another excited triplet molecule are anticipated. Although such interactions are known as T−T annihilation, there has been no observation of the pair constituted by two excited triplet molecules to date. Observation of the pair by TREPR will result in direct and novel information.

Acknowledgment. This work was supported by Grant-in-Aid for Scientific Research on Priority Area "Nanoscale Magnetism and Transport" No. 09236202 from the Ministry of Education, Science, Sports and Culture, Japan.

JA973146F